Adsorption of Dyes from Synthetic Wastewater using Doum Palm Activated Carbon

A.S. Usman[1], M.B. Ibrahim[2] and U. Bishir[2]

[1]*Department of Chemistry, Faculty of Science, Yobe State Unversity, Damaturu, Nigeria*
[2]*Department of Pure and Industrial Chemistry, Faculty of Physical Sciences, College of Natural and Pharmaceutical Sciences, Bayero University, Kano, Nigeria*

ABSTRACT

The adsorption capacity of activated carbon from Doum palm (DP) seed shells on Methylene blue (MB), Methyl orange (MO) and Rhodamine B (RB) dyes was investigated using the batch adsorption method. The adsorbent was characterized by point of zero charge (pH_{PZC}), scanning electron microscopy (SEM) and Fourier transform infrared spectroscopy (FTIR). The effects of operating parameters such as initial dye concentration, adsorbent dosage, contact time, pH and temperature on the adsorption were investigated. The maximum adsorption capacities were found to be 81.81, 73.38 and 88.40 mg/g for MB, MO and RB respectively. The adsorption equilibrium data were analysed using Langmuir, Freundlich and Dubinin-Radushkevich isotherm models and it was revealed that the processes obey the Freundlich model. The adsorption kinetics was studied using pseudo-first order, pseudo-second order and Elovich models and observed that the adsorption of MB, MO and RB follow pseudo-second-order assumptions. The thermodynamic parameters revealed that the adsorption is spontaneous and in most cases endothermic. The results also showed that Doum palm seed shell carbons could be used as a low-cost material to remove anionic and cationic dyes from wastewater.

KEYWORDS

Doum palm, Adsorption, Dye removal, Isotherm, Adsorption kinetics

Received 8 October 2023, revised 11 December 2024, accepted 10 February 2025

INTRODUCTION

Dye-related environmental contamination can seriously harm crops and aquatic species by reducing some of their activities.[1,2] Furthermore, various researchers have shown that depending on the type and physicochemical characteristics of dye molecules, dyes can adversely affect human health and the environment.[3,4] The paper, printing, plastics, and leather industries use a lot of dyes and water in their processes. The wastewater generated from the various activities make these industries one of the major sources of dye pollution.[5-7]

Water treatment techniques to remove colour molecules include ion exchange, coagulation, biodegradation, and precipitation. These techniques have significant limitations which include excessive energy usage, insufficient dye removal, and the production of poisonous sludge.[8] Due to its straightforward operation, high efficiency at removing dye molecules, and adaptability in terms of the characteristics of the adsorbent employed as a separation medium, the adsorption method is a useful technology for removing dye molecules from water.[9-11] Water decolourization has been carried out using a variety of adsorbents.[12-14]

Recently, many studies have focused on the use of inexpensive adsorbent materials for water treatment. Activated carbon (AC) is a highly effective adsorbent for removing heavy metals and dyes from contaminated solutions due to its suitable physical and chemical properties. High specific surface area, multiple surface functional groups, a well-developed internal pore structure, low density, good mechanical strength, ease of regeneration, good chemical and thermal stability, and suitability for large-scale production are the characteristics that make AC unique and efficient. Due to its affordability, abundance, renewability, adequate absorptive qualities, and environmental friendliness,[15–17] AC has recently gained significant attention in wastewater treatment applications.[18,19]

Many studies employ inexpensive and conveniently accessible agricultural solid wastes as adsorbents to extract dyes from wastewater based on their physico-chemical properties.[7] The following are the components of most of the agricultural solid wastes: cellulose, lignin, hemicelluloses, lipids, proteins, etc.[20,16] Additionally, agricultural wastes are abundant and have potentially high adsorption capacity due to the range of functional groups (-OH, -C=O, -C-O, and $-NH_2$) on their surface.[18] Consequently, agricultural solid wastes can be employed as an affordable and environmentally beneficial adsorbent for the removal of dyes from an aqueous solution.[21,18] Several adsorbents such as date stones,[22] Date palm seeds,[23] Microalgal biomass,[24] Coconut shell,[25] Banana roots,[26] Ackee apple pods,[27] Soya wastes,[28] Corncob wastes[29] and Watermelon rind derived from agricultural solid wastes have been employed in various adsorption studies.[30]

In this study, the potential application of Doum palm seed shell activated carbon to remove the Methylene blue, methyl orange and Rhodamine B dyes from synthetic wastewater was investigated. The influence of adsorption parameters including contact time, activated carbon dose, dye initial concentration, temperature and pH were studied. The characterization of the adsorbent before and after adsorption was achieved to identify the mechanism governing the binding of the dye molecules on the adsorbent. Adsorption thermodynamics, isotherm and kinetic studies have been carried out to ascertain the mechanism of the adsorption process.

MATERIALS AND METHODS

The plant materials were washed thoroughly with distilled water to remove any adhering dirt. It was then left to dry under the sun. The dried materials were crushed to powder using a mechanical grinding machine, then washed and rinsed with distilled water and dried in the oven at 105 °C for 6 h.[31]

The activated carbon of DP was prepared by chemical activation using H_3PO_4 (Guangdang Guanghua Chemical Factory Co. Ltd. Shanfau, Guangdang China). The powder of DP was mixed with H_3PO_4 in the ratio 2:1 (activating agent to the substrate) wt/wt., stirred intermittently for 30 min to make a slurry, and dried in an oven (Oven NYC 101) at 110 °C for 24 h. The samples were carbonised in a furnace (p. SLECTA) at 600 °C and a heating rate of 10 °C/min for 1 h. The resulting AC was washed several times with warm deionised water until the pH was constant, then filtered and dried at 110 °C for 24 h.[32,33]

*To whom correspondence should be addressed
Email: abdullerhy135@gmail.com

ISSN 1996-840X Online / South African Chemical Institute / http://saci.co.za/journal

https://doi.org/10.17159/0379-4350/2025/v79a02

The stock solutions of MB, MO and RB dyes (1000 mg/dm^3) were prepared by dissolving known amounts of the dyes in 1000 mL distilled water. These were diluted to the targeted concentrations to be used during the batch adsorption experiment.

The adsorption capacity of the DP activated carbon to remove the dyes from the water was examined using the batch adsorption method under various conditions to determine how some parameters affect the adsorption process. The varied parameters included, contact time (10 to 120 min), adsorbent dose (0.1 to 1 g), initial dye concentration (10 to 100 mg/L), pH of the medium (2 to 12), and system temperature (303.15 to 333.15 K).[34] 100 mL of the dye solutions in conical flasks were agitated at 200 rpm in incubator shaker (Innova 4000, New Brunswick Scientific Co. Inc. Edison, New jersey, USA). After the preset time, the solutions were removed and filtered and the residual dye concentrations were determined from the absorbance of the filtrate using a UV/Vis spectrophotometer (Lambda 35, Perkin Elmer, Milano, Italy). The quantities of the adsorbed dyes were calculated using equation (1).

$$q_e = \frac{(C_i - C_f)}{m} \times V \quad (1)$$

Where q_e (mg/g) is the amount of dye adsorbed, C_i (mg/dm^3) is the initial dye concentration, C_f (mg/dm^3) is the final dye concentration, m (g) is the amount of adsorbent and V (dm^3) is the volume of the aqueous solution.

RESULTS AND DISCUSSION

Characterization

The changes in surface morphology caused by the chemical modification of bio-waste to form activated carbon and subsequent changes brought on by the adsorption of dye are visible in scanning electron microscopy (SEM) measurement (Figure 1). The SEM measurement of DP before activation and H_3PO_4-activated carbons of DP before and after adsorption are shown in Figure 1. The raw plant adsorbent typically appears with a relatively smooth surface, with some natural irregularities and roughness (figure 1a). Deep cavities and irregular pores are visible on the surface of DP-H_3PO_4 which can be identified by uneven hollow ridges (figure 1b). Because of their increased porosity, carbonaceous adsorbents are preferentially chosen for adsorptive processes. However, Figure 1(c) shows that the porous structures, together with the ridges and cavities, are decreased after dye adsorption. It may be caused by dye molecules adsorbing into the pores and cavities of the DP-H_3PO_4 surface, gradually reducing the surface imperfections. A similar morphology pattern has been reported on modified acid-treated activated carbon.[35]

Figure 2 shows the FTIR spectra of DP and its phosphoric acid-activated derivative, DP-H_3PO_4 before and after RB dye adsorption. The presence of broad absorption peaks at 3500–3200 cm^{-1} corresponds to the stretching of hydroxyl groups –OH.[36] The bands obtained 2020–2140 cm^{-1} indicate the stretching of C—C. The presence bands at 1580 and 1600 cm^{-1} are associated with absorption due to cyclic alkene C=C. The presence of the band at 1050 and 1160 cm^{-1} show stretching vibrations of C—O.[37] The Peaks located at 1450 cm^{-1} are assigned to the Alkane bending of C—H. Some changes were observed in the FTIR of the activated carbons before and after the adsorption of RB dye. The intensity of the bands corresponding to –OH stretching vibrations, C≡N groups and C=C cyclic alkene decreased, the band at 1320 cm^{-1} of the DP adsorbent related to –OH bending disappeared, and all of the bands at the region of 1500-1000 cm^{-1} were slightly shifted to the higher wave numbers.

Moisture content, ash content and bulk density

Table 1 represents the bulk density, moisture and ash contents of the adsorbents used in this study. The adsorbents (DP and DP-H_3PO_4) show low moisture contents of 3.72% and 4.28% respectively. The moisture content value depends on the pore volume and surface area of an adsorbent. Therefore, adsorbents with larger pore volumes and surface area tend to absorb more moisture than the ones with less.

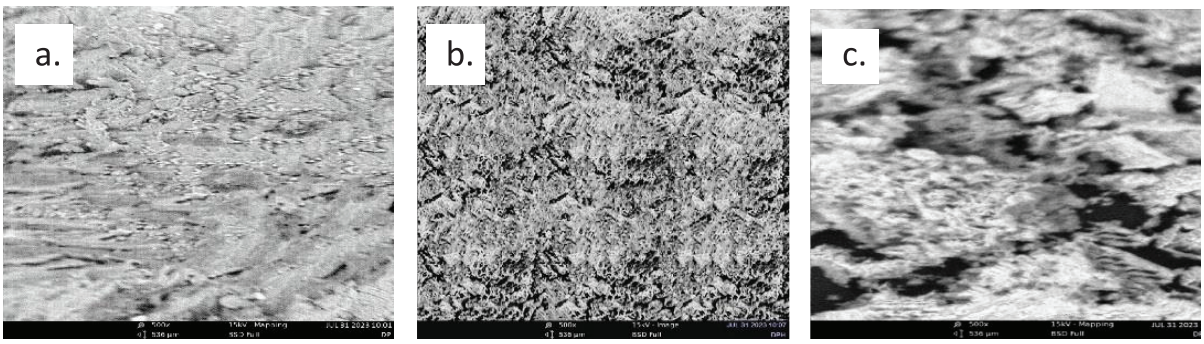

Figure 1: SEM Images of (a) DP, (b) DP-H_3PO_4 before Adsorption and (c) DP-H_3PO_4 after Adsorption

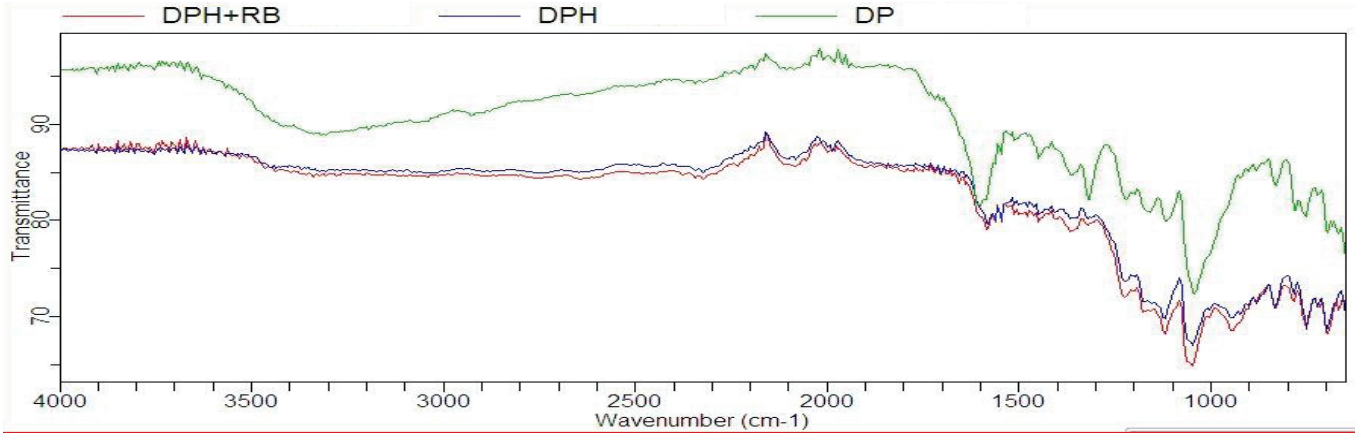

Figure 2: FTIR Spectra of DP and DP-H_3PO_4 before and after RB Adsorption

Table 1: Moisture and ash contents and bulk densities of the adsorbents

S/N	Adsorbent	Moisture Content (%)	Ash Content (%)	Bulk Density (g/cm^3)
1	DP	3.72	18.48	0.69
2	DP-H_3PO_4	4.28	46.83	0.52

The moisture contents found in this study are far less than the value of 11.76% obtained for Coconut fibre.[38]

Ash content shows the level of undesirable inorganic matter whose presence increases the hydrophilic nature and is capable of causing a catalytic effect that leads to restructuring when the activated carbon is regenerated.[39] DP-H_3PO_4 shows high ash content of 46.83%. This reveals that DP-based adsorbents produced more ash at the pyrolysis temperature. This implies that DP-H_3PO_4 would have the least mechanical strength and reduced adsorption capacity due to the covering of the pores of the activated carbons.[40] The ash content for DP and DP-H_3PO_4 are greater than the 15.30 % reported in a study on the adsorption of methylene blue from textile industrial wastewater onto activated carbon of *Parthenium hysterophorus*.[41]

The bulk density of an adsorbent shows its tendency for agglomeration. Adsorbents with higher bulk densities tend to agglomerate more easily. In this study, DP is the carbon precursor and shows a bulk density of 0.69 g/cm^3. In the same vein, the acid-activated derivative carbon DP-H_3PO_4 exhibits a bulk density of 0.52 g/cm^3. Furthermore, this reveals that precursors with higher bulk densities produce denser activated carbons and that acid activation reduces the density of the biomaterial. The bulk density for the biosorbent and acid-derived activated carbon are 0.25 and 0.08 g/cm^3 higher than previously reported.[42]

Point of Zero Charge (pH_{PZC})

The pH_{PZC} analysis was carried out on the prepared adsorbents to determine the pH values where the surface of the adsorbents carries no charge as presented in Figure 3.

Figure 3 shows the plot of change in pH against initial pH and the pH_{PZC} for the he activated carbon and its precursor. pH_{PZC} is the point at which the surface charge generated on the adsorbent is zero.[32] The DP and DP-H_3PO_4 adsorbent show values between 7.10 and 7.30 respectively. The adsorbents with low pH_{PZC} have high affinity to cationic molecules while those with high pH_{PZC} tend to bind more with anionic molecules.[34] Furthermore, at a pH lower than pH_{PZC}, the surface of the adsorbents is protonated which in turn favours the removal of anionic dyes solution. On the other hand, if the pH of the system is greater than pH_{PZC}, the surface of the adsorbents is deprotonated which exposes negative sites thereby favouring the removal of cationic dyes owing to the presence of OH^- groups.

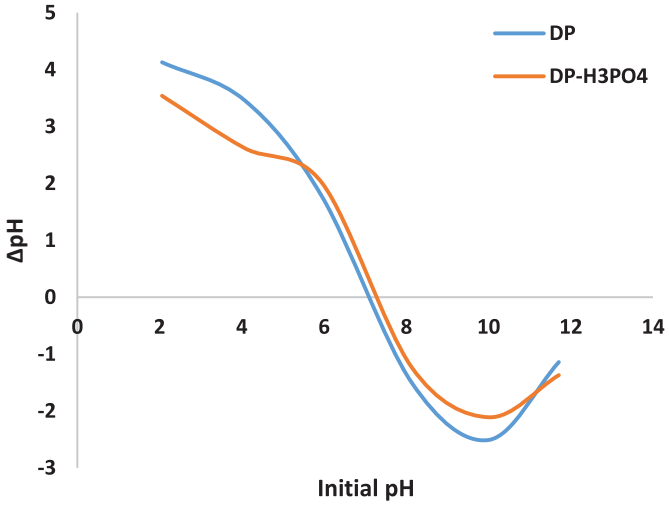

Figure 3: pH_{PZC} of unactivated DP and activated DP-H_3PO_4

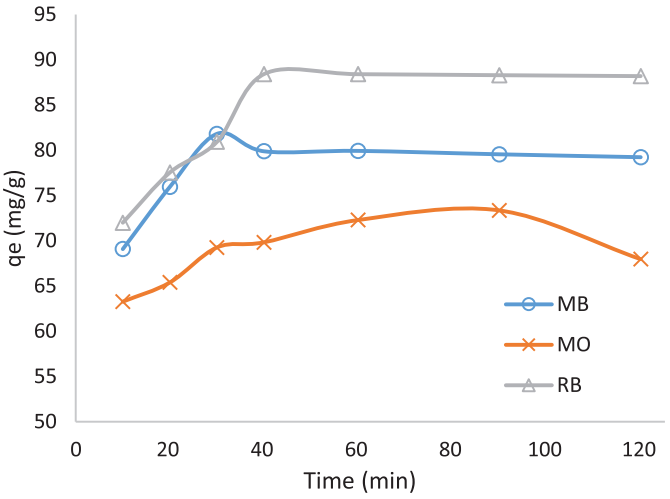

Figure 4: Effect of Contact Time on the Removal of MB, MO and RB using DP-H_3PO_4

Batch adsorption studies

Effect of contact time

The rate of dye adsorption depends on the time that an adsorbent spends in contact with the dyes. In this study, this was ascertained by adding a constant dosage of the adsorbents in 100 mg/L of the MB, MO and RB solutions. The mixtures were agitated and analyzed for residual dye concentration at time intervals of 10, 20, 30, 40, 60, 90 and 120 min. The adsorptive behaviours of MB, MO and RB on DP-H_3PO_4 was analysed in Figure 4. The result indicated that the removal of the three dyes increased with time. RB was removed the most with a removal amount of 88.42 mg/g after 40 min. Second in the removal order was MB with 81.81 mg/g after 30 min whereas 73.35 mg/g of MO was removed at 90 min. The adsorption rate was rapid in the removal of RB and very slow in the case of MO. The order of removal of the dyes favoured the cationic dyes placing RB highest then MB and MO in that order. This trend could be attributed to the prevalence of negative charges on the adsorbent surface. A similar result was reported.[43]

Effect of adsorbent dose

To test the influence of adsorbent dosage on the removal of MB, MO and RB from water, various mass of the adsorbents (from 0.1 to 1 g) were agitated with 100 cm^3 of 20 mg/L solutions of the dye the solutions. The variation in the amount of dye removal with DP-H_3PO_4 dosage is shown in Figure 5. The graph shows that the adsorption capacity for MB, MO and RB decreases with an increase in the dosage of DP-H_3PO_4. This might be due to the increase in the aggregation of the adsorbent thereby reducing the surface area availability of the active sites. The highest removed dye was MB at 15.43 mg/g followed by MO and RB with 14.32 and 9.35 mg/g respectively. The adsorption trend is consistent with previous findings of an optimum dosage of 0.35 g/100 cm^3.[44] The pattern of this result is contrary to the findings with an optimum dosage of 0.8 g/100 cm^3 for MB and 2 g/100 cm^3 for Congo red (CR) dye.[45]

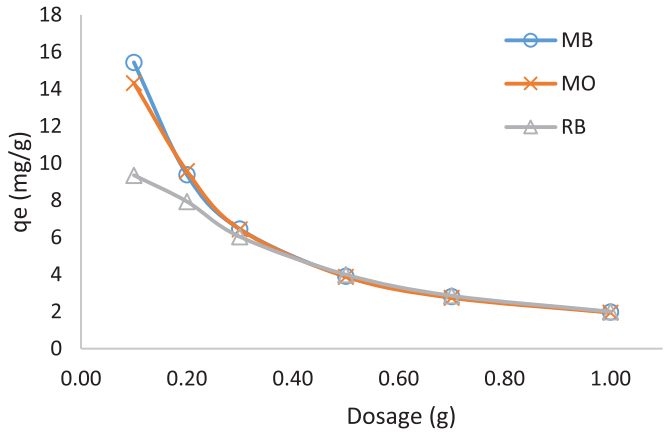

Figure 5: Effect of DP-H_3PO_4 dosage on the removal of MB, MO and RB from water

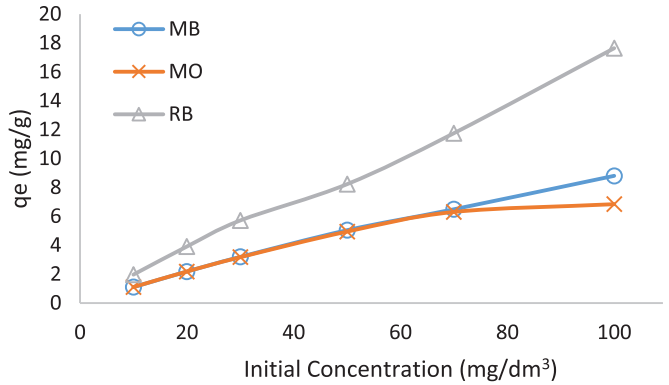

Figure 6: Effect of Dye Initial Concentration on the Adsorption of MB, MO and RB onto DP-H_3PO_4

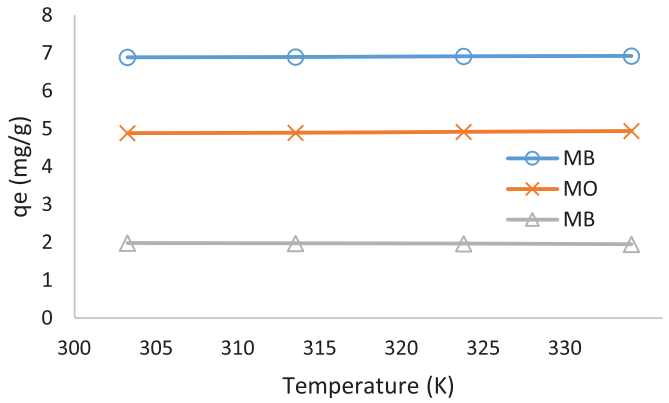

Figure 7: Effect of temperature on the adsorption of MB, MO and RB onto DP-H_3PO_4

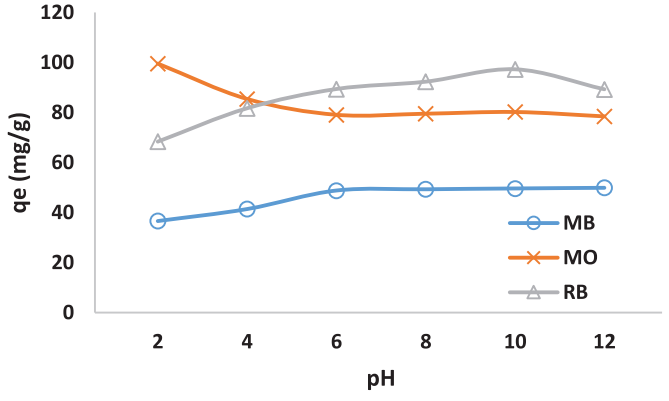

Figure 8 Effect of solution pH on the adsorption of MB, MO and RB onto DP-H_3PO_4

Effect of initial dye concentration

The influence of initial dye concentration was studied by varying the concentrations of MB, MO and RB from 10 to 100 mg/dm³ and agitated with the optimum dosages of the adsorbents for the optimum time previously obtained. Figure 6 shows the influence of initial concentrations of MB, MO and RB on their removals by DP-H_3PO_4 sorbent. The result reveals that the removal of MB MO and RB increases with increase in the initial concentrations of the dyes. The adsorption capacity for MB hiked from 1.10 to 8.80 mg/g when its initial concentration increased from 10 to 100 mg/dm³. The removal of MO and RB also followed the same trend, increasing from 1.10 and 1.97 mg/g at initial concentrations of 10 mg/dm³ to 6.84 and 17.64 mg/g respectively at initial concentrations of 100 mg/dm³. The high adsorption capacity of the dyes at high initial concentrations could be attributed to the availability of active adsorption sites and their increased interaction with the dye molecules.[46] This trend is in agreement with those described for the removal of Acriflavine, and Victoria blue B by Indian jujube-based activated carbon.[47]

Effect of temperature

The variation in the adsorbed amount of MB, MO and RB are analysed at varying temperatures of 303.15, 313.15, 323.15 and 333.15 K, while other influencing parameters such as contact time, adsorbent dosage and initial dye concentrations are kept constant at predetermined optimum values. The results of the investigation on the variation of adsorption of MB, MO and RB with temperature using DP-H_3PO_4 as adsorbent is depicted in Figure 7. The outcome reveals that the adsorption capacities of MB and MO increased from 6.88 and 4.88 mg/g at 303.15 K to 6.92 and 4.94 mg/g at 333.15 K respectively. This trend could be ascribed to the increase in the mobility of the MB and MO dye ions with an increase in temperature.[48] It could also be due to a decrease in the viscosity of the solution which results in the increase in the surface activity of MB and MO which consequently accelerates their diffusion rate on the adsorbent channels. On the other hand, the adsorption rate for RB remains almost steady when the temperature increases from 303.15 K to 333.15 K. It could be explained by a steady interaction between RB molecules and the active sites of DP-H_3PO_4 adsorbent.[49] Similar finding has been reported on the adsorption dyes using magnetic N-rich activated carbon derived from egg white biomass and sucrose.[50]

Effect of pH

Solution pH is a key factor influencing the capacity of adsorbents to remove organic dyes from wastewater. As one of the main mechanisms of adsorption, electrostatic attraction between adsorbent and adsorbate is related to the solution pH. The solution pH also determines the chemical speciation of the dye molecules as well as the ionization of oxygen-containing functional groups on the surface of the adsorbent.[51] The influence of solution pH on the adsorption of MB, MO and RB onto DP-H_3PO_4 was investigated. This was achieved by varying the pH of the solution in the range of 2 to 12 keeping other parameters like contact time, adsorption dosage, initial dye concentration and temperature constant at the predetermined optimum values. The influence of pH on the adsorption of MB, MO and RB is shown in Figure 8. It is evident from the result that the adsorption of MB and RB increased with an increase in pH while that of MO decreased in the same direction. The adsorption capacity for MB increases from 36.59 mg/g at pH 2 to 49.89 mg/g at pH 12. The removal rate of RB increased from 68.35 mg/g at pH 2 to 97.27 mg/g at pH 10. Whereas the adsorption of MO declined from 99.54 to 79.06 mg/g when the solution pH was raised from 2 to 6. It can be deduced that the adsorbent shows high affinity for the cationic MB and RB dyes at high pH values and for anionic MO at low pH values. This might be because, as pH increases, the active groups of DP-H_3PO_4 are deprotonated which increases the negative charge density and in

return, the cationic RB and MB are actively attracted. The reverse is the case for MO where at low pH the surface of the adsorbent becomes highly protonated increasing its affinity for the MO molecules. The adsorption pattern obtained here corresponds with the report on the adsorption of Direct Red 4BS, N Acid Orange II, N React Blue 19, and N Methylene Blue onto sludge-rice husk biochar.[52]

Thermodynamic studies

Table 2 shows the thermodynamic parameters for the adsorption of MB, MO and RB onto DP, DP-H_3PO_4 adsorbent. The results show that all the ΔG values are negative indicating the spontaneity of the adsorption of MB, MO and RB onto all the adsorbents. When the temperature increased from 303.15 to 333.15 K, the magnitudes of ΔG increased its negativity which reveals the increase in the spontaneity of the adsorption processes with the rise in temperature except for RB where the negativity decreases. The values of enthalpy change are found to be positive in the adsorption of MB and MO revealing that the processes are endothermic. Nevertheless, negative ΔH values were obtained for the uptake of RB hence the process is considered exothermic. The ΔH values for the adsorption of MB and MO are less than 20.9 $kJmol^{-1}$ indicating that the adsorptions are driven predominantly by physisorption. The sorption of RB shows a ΔH of -27.92 thus the processes are attributed to chemisorption.[54] It is evident from the result that ΔS values are positive indicating the increase in randomness at the solid/liquid interface.[55] The cause of this could be attributed to water molecules being liberated as a result of molecular exchange between dye molecules and functional groups on the adsorbent surface, which led to greater irregularity at the solid/fluid boundary.[56] The negative ΔS value is observed in RB adsorption which indicates a decrease in randomness at the adsorbent/liquid interface.[57] The observed behaviours of the thermodynamic parameters are similar to the Study on the adsorption of dyestuffs with different properties by sludge-rice husk biochar[52] and the adsorption of organic dyes by $HDPy^+$-modified clay.[58]

Adsorption kinetics

Pseudo-first order (PFO), Pseudo-second order (PSO) and Elovich models were investigated. Table 3 represents the PFO, PSO and Elovich model parameters for the adsorption of MB, MO and RB using DP-H_3PO_4. It is evident from the result that the model that gave the best fit for the adsorption of MB, MO and RB onto DP-H_3PO_4 is PSO. This is indicated by the R^2 values of 0.9996, 0.9962 and 0.9994 for the fitting of MB, MO and RB data respectively. In addition, the calculated qe values obtained by PSO (80.00, 70.42 and 90.90 mgg^{-1}) are more concordant with the experimental values (81.81, 73.34 and 88.42) than the values obtained by PFO. This corroborates the fact that the process is best described by the PSO model. Moreover, the PSO rate constant (k_2) and the initial adsorption rates (h) calculated are found to be in the order MO > MB > RB. The data for MB, MO and RB adsorption also show good fitting with the Elovich model with R^2 values of 0.9893, 0.9702 and 0.9187 respectively. The desorption constant, β as indicated by the Elovich model is in the order MO > RB > MB. The result obtained here corresponds with the report on the adsorption of cationic dyes onto H_3PO_4-activated *Ziziphus Mauritania* seeds.[47]

Adsorption isotherms

Adsorption isotherms explain the dye molecule distribution between solid phase and bulk solution. In the equilibrium state, a certain relationship exists between the concentration of solute in the solution and the amount of solute adsorbed by the adsorbent under the fixed conditions.[59] It also provides information on the surface properties and adsorption behaviour of the adsorbent and helps to study the adsorption mechanism.[60] The adsorption data was analyzed by fitting to Freundlich, Langmuir and Dubinin-Radushkevich isotherm models. The Langmuir, Freundlich and Dubinin-Radushkevich isotherm parameters for the adsorption of MB, MO and RB onto DP-H_3PO_4 are evaluated and shown in Table 4. The result shows that the highest R^2 values for MB and MO (0.9943 and 0.9853 respectively) obtained by the Freundlich model imply that the adsorptions of MB and MO are best described by the Freundlich isotherm. The K_F values obtained show that the adsorption capacities are in the order MB > MO. On the other hand, the extent of heterogeneity and adsorption favourability as indicated by the n parameter are 2.7663 and 3.5829 for MB and MO respectively. This implies that the adsorption of MO is more favourable and heterogeneous than MB. Langmuir model exhibits the best fitting in the experimental data for RB adsorption

Table 2: Thermodynamic Parameters for the Adsorption of MB, MO and RB onto DP-H_3PO_4

Adsorbent	Dye	ΔH (kJ/mol)	ΔS (kJ/mol.K)	ΔG (kJ/mol)			
				303.15 K	313.15 K	323.15 K	333.15 K
DP-H_3PO_4	MB	11.7751	0.0537	-4.5011	-5.0380	-5.5749	-6.1118
	MO	19.2644	0.0750	-3.4811	-4.2314	-4.9817	-5.7320
	RB	-27.9234	-0.0661	-7.8903	-7.2295	-6.5687	-5.9078

Table 3: Kinetic model parameters for the adsorption of MB, MO and RB onto DP-H_3PO_4

S/N	Kinetics Model	Parameters	Values		
			MB	MO	RB
1	Pseudo-First Order	q_e (mgg^{-1})	169.2388	19.5524	50.5825
		K_1 (min^{-1})	0.2119	0.0468	0.0762
		R^2	0.8795	0.9867	0.8320
2	Pseudo-Second Order	q_e (mgg^{-1})	80.0000	70.4225	90.9091
		k_2 ($gmg^{-1}min^{-1}$)	0.0256	0.0672	0.0044
		h ($mgg^{-1}min^{-1}$)	163.9344	333.3333	36.1011
		R^2	0.9996	0.9962	0.9994
3	Elovich model	α ($mgg^{-1}min^{-1}$)	472.8719	190921.8826	716.6898
		β (gmg^{-1})	0.0876	0.2042	0.0913
		R^2	0.9893	0.9702	0.9187

Table 4: Isotherm Parameters for the Adsorption of MB, MO and RB onto DP-H_3PO_4

S/N	Isotherms	Parameters	Values		
			MB	MO	RB
1	Langmuir	q_{max} (mgg^{-1})	5.1361	4.3535	10.3950
		K_L (Lmg^{-1})	3.1302	7.7864	1.5417
		R^2	0.9451	0.9068	0.9695
2	Freundlich	K_F (Lmg^{-1})	2.8783	2.8383	4.7394
		N	2.7663	3.5829	2.4722
		R^2	0.9943	0.9853	0.9205
3	Dubinin-Radushkevich	q_s ($molg^{-1}$)	5.2409	4.6791	9.7806
		β (mol^2kJ^{-2})	0.0409	0.0237	0.0654
		E ($kJmol^{-1}$)	3.4964	4.5932	2.7650
		R^2	0.7640	0.7547	0.7680

onto DP-H_3PO_4. This is indicated by the higher R^2 value of 0.9695 as compared to 0.9205 and 0.7680 obtained by Freundlich and Dubinin-radushkevich models respectively. This reveals that RB adsorbed in monolayer onto energetically homogenous active sites of DP-H_3PO_4 with the absence of mutual interaction between the dye molecules. The values of the R_L parameter (0.0298 – 0.0031) show that the adsorption process is favourable. Freundlich form adsorption similar to this was reported in a study on the uptake of reactive blue 19 and reactive red 218.[61] The Langmuir model fitting was also reported.[35]

CONCLUSIONS

In this study, activated carbon (DP-H_3PO_4) was prepared from Doum palm seed shell using H_3PO_4. The SEM analysis reveals irregular porous structures; whereas the FTIR results show oxygen-containing functional groups on the surface of the activated carbon. The maximum adsorption capacity for MB, MO and RB dyes was obtained after the contact time of 30, 40 and 90 min respectively. The uptake of MO dye is enhanced at acidic pH while the adsorption of MB and RB are enhanced at basic pH. The adsorption capacities of all the dyes increased with the increase in their initial concentration and decrease with an increase in the adsorbent dosage. The maximum adsorption corresponds with the calculated values obtained by the pseudo-second-order (PSO) kinetic model. The thermodynamic studies show that the adsorption of all the dyes is spontaneous as indicated by the negative ΔG. However, ΔH values are positive for MB and MO indicating endothermic adsorption and negative for RB which indicates exothermic adsorption. Kinetic studies revealed that the adsorption process follows the PSO model whereas the adsorption isotherm study indicates that the process follows the Freundlich model. It is evident from the result that Doum palm-activated carbon can serve as a plausible adsorbent for the removal of dyes from wastewater.

ACKNOWLEDGEMENTS

The authors express their heartfelt gratitude to Tertiary Education Trust Fund (TETFund), Bayero University Kano and Yobe State University Damaturu.

ORCID IDS

A.S. Usman: https://doi.org/0009-0001-0083-8861
M.B. Ibrahim: https://doi.org/0000-0001-7581-7937
U. Bishir: https://doi.org/0000-0002-1738-4368

REFERENCES

1. Rovani S, Fernandes AN, Prola LDT, Lima EC, Santos WO, Adebayo MA. Removal of Cibacron Brilliant Yellow 3G-P Dye from Aqueous Solutions by Brazilian Peats as Biosorbents. Chem Eng Commun. 2014;201(11):1431–1458. https://doi.org/10.1080/00986445.2013.816954.
2. Bazzo A, Adebayo MA, Dias SLP, Lima EC, Vaghetti JCP, de Oliveira ER, Leite AJB, Pavan FA. Avocado seed powder: characterization and its application for crystal violet dye removal from aqueous solutions. Desalination Water Treat. 2016;57(34):15873–15888. https://doi.org/10.1080/19443994.2015.1074621.
3. Adebayo MA, Prola LDT, Lima EC, Puchana-Rosero MJ, Cataluna R, Saucier C, Umpierres CS, Vaghetti JCP, da Silva LG, Ruggiero R. Adsorption of Procion Blue MX-R dye from aqueous solutions by lignin chemically modified with aluminium and manganese. J Hazard Mater. 2014;268:43–50. https://doi.org/10.1016/j.jhazmat.2014.01.005.
4. Ribas MC, Adebayo MA, Prola LDT, Lima EC, Cataluna R, Feris LA, Puchana-Rosero MJ, Machado FM, Pavan FA, Calvete T. Comparison of a homemade cocoa shell activated carbon with commercial activated carbon for the removal of reactive violet 5 dye from aqueous solutions. Chem Eng J. 2014;248:315–326. https://doi.org/10.1016/j.cej.2014.03.054.
5. Pang X, Sellaoui L, Franco D, Dotto GL, Georgin J, Bajahzar A, Belmabrouk H, Ben Lamine A, Bonilla-Petriciolet A, Li Z. Adsorption of crystal violet on biomasses from pecan nutshell, para chestnut husk, araucaria bark and palm cactus: experimental study and theoretical modelling via monolayer and double layer statistical physics models. Chem Eng J. 2019;378:122101. https://doi.org/10.1016/j.cej.2019.122101.
6. Li Z, Sellaoui L, Dotto GL, Lamine AB, Bonilla-Petriciolet A, Hanafy H, Belmabrouk H, Netto MS, Erto A. Interpretation of the adsorption mechanism of Reactive Black 5 and Ponceau 4R dyes on chitosan/polyamide nanofibers via advanced statistical physics model. J Mol Liq. 2019;285:165–170. https://doi.org/10.1016/j.molliq.2019.04.091.
7. Gupta VK, Suhas. Application of low-cost adsorbents for dye removal – A review. J Environ Manage. 2009;90(8):2313–2342. https://doi.org/10.1016/j.jenvman.2008.11.017.
8. de Luna MDG, Flores ED, Genuino D A D, Futalan CM, Wan MW. Adsorption of Erichrome Black T (EBT) dye using activated carbon prepared from waste rice hulls-optimization, isotherm and kinetic studies. J Taiwan Inst Chem Eng. 2013;44(4):646–653. https://doi.org/10.1016/j.jtice.2013.01.010.
9. Da'na E. Adsorption of heavy metals on functionalized-mesoporous silica: A review. Microporous Mesoporous Mater. 2017;247:145–157. https://doi.org/10.1016/j.micromeso.2017.03.050.
10. Peng W, Li H, Liu Y, Song S. A review on heavy metal ions adsorption from water by graphene oxide and its composites. J Mol Liq. 2017;230:496–504. https://doi.org/10.1016/j.molliq.2017.01.064.
11. Sherlala AIA, Raman A A A, Bello MM, Asghar A. A review of the applications of organofunctionalized magnetic graphene oxide nanocomposites for heavy metal adsorption. Chemosphere. 2018;193:1004–1017. https://doi.org/10.1016/j.chemosphere.2017.11.093.
12. Gupta VK, Mittal A, Kurup L, Mittal J. Adsorption of a hazardous dye, erythrosine, over hen feathers. J Colloid Interface Sci. 2006;304(1):52–57. https://doi.org/10.1016/j.jcis.2006.08.032.

13. Bello OS, Auta M, Ayodele OB. Ackee apple (*Blighia sapida*) seeds: a novel adsorbent for the removal of Congo red dye from aqueous solutions. Chem Ecol. 2013;29(1):58–71. https://doi.org/10.1080/02757540.2012.686606.
14. Bello OS, Ahmad MA. Coconut (*Cocos nucifera*) Shell Based Activated Carbon for the Removal of Malachite Green Dye from Aqueous Solutions. Sep Sci Technol. 2012;47(6):903–912. https://doi.org/10.1080/01496395.2011.630335.
15. Shokry H, Elkady M, Hamad H. Elkady, Hamad H. Nano activated carbon from industrial mine coal as adsorbents for removal of dye from simulated textile wastewater: operational parameters and mechanism study. J Mater Res Technol. 2019;8(5):4477–4488. https://doi.org/10.1016/j.jmrt.2019.07.061.
16. Gupta VK, Saleh TA. Sorption of pollutants by porous carbon, carbon nanotubes and fullerene—an overview. Environ Sci Pollut Res Int. 2013;20(5):2828–2843. https://doi.org/10.1007/s11356-013-1524-1.
17. Lugo-Lugo V, Hernández-López S, Barrera-Díaz C, Ureña-Núñez F, Bilyeu B. A comparative study of natural, formaldehyde-treated and copolymer-grafted orange peel for Pb(II) adsorption under batch and continuous mode. J Hazard Mater. 2009;161(2-3):1255–1264. https://doi.org/10.1016/j.jhazmat.2008.04.087.
18. Gupta VK, Nayak A, Bhushan B, Agarwal S. A critical analysis on the efficiency of activated carbons from low-cost precursors for heavy metals remediation. Crit Rev Environ Sci Technol. 2015;45(6):613–668. https://doi.org/10.1080/10643389.2013.876526.
19. Lorenc-Grabowska E, Gryglewicz G, Machnikowski J. p-Chlorophenol adsorption on activated carbons with basic surface properties. Appl Surf Sci. 2010;256(14):4480–4487. https://doi.org/10.1016/j.apsusc.2010.01.078.
20. Ashrafi SD, Kamani H, Jaafari J, Mahvi AH. Experimental Design and Response Surface Modeling for Optimization of Fluoroquinolone Removal from Aqueous Solution by NaOH-Modified Rice Husk. Desalination Water Treat. 2016;57(35):16456–16465. https://doi.org/10.1080/19443994.2015.1080188.
21. Bhatnagar A, Sillanpää M, Witek-Krowiak A. Agricultural Waste Peels as Versatile Biomass for Water Purification - A Review. Chem Eng J. 2015;270:244–271. https://doi.org/10.1016/j.cej.2015.01.135.
22. Foo KY, Hameed BH. Preparation of activated carbon from date stones by microwave-induced chemical activation: application for methylene blue adsorption. Chem Eng J. 2011;170(1):338–341. https://doi.org/10.1016/j.cej.2011.02.068.
23. Islam MA, Tan I A W, Benhouria A, Asif M, Hameed BH. Mesoporous and adsorptive properties of palm date seed activated carbon prepared via sequential hydrothermal carbonization and sodium hydroxide activation. Chem Eng J. 2015;270:187–195. https://doi.org/10.1016/j.cej.2015.01.058.
24. Yu KL, Lee XJ, Ong HC, Chen W-H, Chang J-S, Lin C-S, Show PL, Ling TC. Adsorptive removal of cationic methylene blue and anionic Congo red dyes using wet-torrefed microalgal biochar: Equilibrium, kinetic and mechanism modelling. Environ Pollut. 2021;272:115986. https://doi.org/10.1016/j.envpol.2020.115986.
25. Yağmur HK, Kaya I. Synthesis and characterization of magnetic ZnCl2-activated carbon produced from coconut shell for the adsorption of methylene blue. J Mol Struct. 2021;1232:130071. https://doi.org/10.1016/j.molstruc.2021.130071.
26. Paluri P, Ahmad KA, Durbha KS. Importance of estimation of optimum isotherm model parameters for adsorption of methylene blue onto biomass-derived activated carbons: comparison between linear and non-linear methods. Biomass Convers Biorefin. 2020;12:4031–4048. https://doi.org/10.1007/s13399-020-00867-y
27. Bello MO, Abdus-Salam N, Adekola FA, Pal U. Isotherm and kinetic studies of adsorption of methylene blue using activated carbon from ackee apple pods. Chemical Data Collections. 2021;31:100607. https://doi.org/10.1016/j.cdc.2020.100607.
28. Batool A, Valiyaveettil S. Chemical transformation of soya waste into stable adsorbent for enhanced removal of methylene blue and neutral red from water. J Environ Chem Eng. 2021;9(1):104902. https://doi.org/10.1016/j.jece.2020.104902.
29. Zhou D, Li D, Li A, Qi M, Cui D, Wang H, Wei H. Activated carbons prepared via reflux-microwave-assisted activation approach with high adsorption capability for methylene blue. J Environ Chem Eng. 2021;9(1):104671. https://doi.org/10.1016/j.jece.2020.104671.
30. Masoudian N, Rajabi M, Ghaedi M. Titanium oxide nanoparticles loaded onto activated carbon prepared from bio-waste watermelon rind for the efficient ultrasonic-assisted adsorption of congo red and phenol red dyes from wastewaters. Polyhedron. 2019;173:114105. https://doi.org/10.1016/j.poly.2019.114105.
31. Alabi AH, Oladele EO, Adeleke AJO, Oni FC, Olanrewaju CA. Equilibrium, Kinetic and Thermodynamic Studies of Biosorption of Methylene Blue on Goethite Modified Baobab Fruit Pod (*Adansonia digitata* L.). J Appl Sci Environ Manag. 2020;24(7):1229–1243. https://doi.org/10.4314/jasem.v24i7.16.
32. Shehu A, Ibrahim MB. Adsorption and Desorption Studies of Dyes onto Pyrolysed Chemically Activated Shea Butter (*Vitellaria paradoxa*). Bayero J Pure Appl Sci. 2022;13(1):283–290.
33. Gaya UI, Otene E, Abdullah A. Adsorption of Aqueous Cd(II) and Pb(II) on Activated Carbon Nanopores Prepared by chemical activation of Doum Palm Shell. Springerplus. 2016;4:458. https://doi.org/10.1186/s40064-015-1256-4
34. Ayuba AM, Sani M. Removal of Eriochrome Black T Dye from Aqueous Solution using Base Activated Typha Grass (*Typha Latifolia*) as an Adsorbent. Bayero J Pure Appl Sci. 2022;15(1):95–104. https://doi.org/10.4314/bajopas.v15i1.13.
35. Patra C, Gupta R, Bedadeep D, Narayanasamy S. Surface Treated Acid-Activated Carbon for Adsorption of Anionic Azo Dyes from Single and Binary Adsorptive Systems: A detail insight. Environ Pollut. 2020;266:115102. https://doi.org/10.1016/j.envpol.2020.115102.
36. Shams Khorramabadi G, Darvishi Cheshmeh Soltani R, Rezaee A, Khataee AR, Jonidi Jafari A. Utilisation of Immobilised Activated Sludge for the Biosorption of Chromium (VI). Can J Chem Eng. 2012;90(6):1539–1546. https://doi.org/10.1002/cjce.20661.
37. Ma X, Ouyang F. Adsorption Properties of Biomass-Based Activated Carbon Prepared with Spent Coffee Grounds and Pomelo Skin by Phosphoric Acid Activation. Appl Surf Sci. 2013;268:566–570. https://doi.org/10.1016/j.apsusc.2013.01.009.
38. Ohimor EO, Temisa DO, Ononiwu PI. Production of Activated Carbon from Carbonaceous Agricultural Waste Material: Coconut Fibres. Nigerian Journal of Technology. 2021;40(1):19–24. https://doi.org/10.4314/njt.v40i1.4.
39. Nedjai R, Alkhatib M F R, Alam MZ, Kabbashi NA. Adsorption of Methylene Blue onto Activated Carbon Dveloped from Baobab Fruit Shell by Chemical Activation: Kinetic Equilibrium Study, IIUM. Eng J (NY). 2021;22(2):31–49.
40. Budianto A, Kusdarini E, Effendi SSW, Aziz M. The Production of Activated Carbon from Indonesian Mangrove Charcoal, IOP Conf. Series: Materials Science and Engineering, 2019;462:012006. https://doi.org/10.1088/1757-899X/462/1/012006.
41. Fito J, Tibebu S, Nkambule TTI. Optimization of Cr (VI) Removal from Aqueous Solution with Activated Carbon Derived from *Eichhornia crassipes* under Response Surface Methodology. BMC Chem. 2023;17(1):4. https://doi.org/10.1186/s13065-023-00913-6.
42. Adebayo GB, Adegoke HI, Fauzeeyat S. Adsorption of Cr(VI) ions onto goethite, activated carbon and their composite: kinetic and thermodynamic studies. Appl Water Sci. 2020;10(9):213. https://doi.org/10.1007/s13201-020-01295-z.
43. Boudechiche N, Fares M, Ouyahia S, Yazid H, Trari M, Sadaoui Z. Comparative Study on Removal of Two Basic Dyes in Aqueous Medium by Adsorption using Activated Carbon from Ziziphus lotus Stones. Microchem J. 2019;146:1010–1018. https://doi.org/10.1016/j.microc.2019.02.010.
44. Jain SN, Tamboli SR, Sutar DS, Jadhav SR, Marathe JV, Shaikh AA, Prajapati AA. Batch and continuous studies for adsorption of anionic dye onto waste tea residue: Kinetic, equilibrium, breakthrough and reusability studies. J Clean Prod. 2020;252:119778. https://doi.org/10.1016/j.jclepro.2019.119778.
45. El Khomri M, El Messaoudi N, Dbik A, Bentahar S, Lacherai A, Chegini ZG, Iqbal M. Organic Dyes Adsorption on the Almond Shell (*Prunus dulcis*) as Agricultural Solid Waste from Aqueous Solution in Single and Binary Mixture Systems. Biointerface Res Appl Chem. 2021;12(2):2022–2040. https://doi.org/10.33263/BRIAC122.20222040.
46. Noreen S, Khalid U, Ibrahim SM, Javed T, Ghani A, Naz S, Iqbal M. ZnO, MgO and FeO Adsorption Efficiencies for Direct Sky Blue Dye: Equilibrium, Kinetics and Thermodynamics Studies. J Mater Res Technol. 2020;9(3):5881–5893. https://doi.org/10.1016/j.jmrt.2020.03.115.

47. Khan TA, Nouman MD, Dua D, Khan SA, Alharthi SS. Adsorptive Scavenging of Cationic Dyes from Aquatic Phase by H_3PO_4 Activated Indian Jujube (*Ziziphus mauritiana*) Seeds based Activated Carbon: Isotherm, Kinetics, and Thermodynamic Study. J Saudi Chem Soc. 2022;26(2):101417. https://doi.org/10.1016/j.jscs.2021.101417.
48. El-Harby NF, Ibrahim SMA, Mohamed NA. Adsorption of Congo Red Dye onto Antimicrobial Terephthaloyl Thiourea Cross-Linked Chitosan Hydrogels. Water Sci Technol. 2017;76(10):2719–2732. https://doi.org/10.2166/wst.2017.442.
49. Sharma K, Sharma S, Sharma V, Mishra PK, Ekielski A, Sharma V, Kumar V. Methylene Blue Dye Adsorption from Wastewater Using Hydroxyapatite/Gold Nanocomposite: Kinetic and Thermodynamics Studies. Nanomaterials (Basel). 2021;11(6):1403. https://doi.org/10.3390/nano11061403.
50. Vahdati-Khajeh S, Zirak M, Tejrag RZ, Fathi A, Lamei K, Eftekhari-Sis B. Biocompatible Magnetic N-rich Activated Carbon from Egg White Biomass and Sucrose: Preparation, Characterization and Investigation of Dye Adsorption Capacity from Aqueous Solution. Surf Interfaces. 2019;15:157–165. https://doi.org/10.1016/j.surfin.2019.03.003.
51. Garba ZN, Zhou W, Lawan I, Xiao W, Zhang M, Wang L, Chen L, Yuan Z. An Overview of Chlorophenols as Contaminants and their Removal from Wastewater by Adsorption: a Review. J Environ Manage. 2019;241:59–75. https://doi.org/10.1016/j.jenvman.2019.04.004.
52. Chen S, Qin C, Wang T, Chen F, Li X, Hou H, Zhou M. Study on the Adsorption of Dyestuffs with Different Properties by Sludge-Rice Husk Biochar: Adsorption Capacity, Isotherm, Kinetic, Thermodynamics and Mechanism. J Mol Liq. 2019;285:62–74. https://doi.org/10.1016/j.molliq.2019.04.035.
53. Subbaiah MV, Kim DS. Adsorption of Methyl Orange from Aqueous Solution by Aminated Pumpkin Seed Powder: Kinetics, Isotherms, and Thermodynamic Studies. Ecotoxicol Environ Saf. 2016;128:109–117. https://doi.org/10.1016/j.ecoenv.2016.02.016.
54. Andelescu A, Nistor MA, Muntean SG, Rădulescu-Grad ME. Adsorption Studies on Copper, Cadmium, and Zinc Ion Removal from Aqueous Solution using Magnetite/Carbon Nanocomposites. Sep Sci Technol. 2018;53(15):2352–2364. https://doi.org/10.1080/01496395.2018.1457696.
55. Luo Z, Gao M, Ye Y, Yang S. Modification of Reduced-charge Montmorillonites by a Series of Gemini Surfactants: Characterization and Application in Methyl Orange Removal. Appl Surf Sci. 2015;324:807–816. https://doi.org/10.1016/j.apsusc.2014.11.043.
56. Bu R, Chen F, Li J, Li W, Yang F. Adsorption Capability for Anionic Dyes on 2-Hydroxyethylammonium Acetate-Intercalated Layered Double Hydroxide. Colloids Surf A Physicochem Eng Asp. 2016;511:312–319. https://doi.org/10.1016/j.colsurfa.2016.10.015.
57. Olusegun SJ, Mohallem ND. Comparative Adsorption Mechanism of Doxycycline and Congo Red using Synthesized Kaolinite Supported $CoFe_2O_4$ Nanoparticles. Environ Pollut. 2020;260:114019. https://doi.org/10.1016/j.envpol.2020.114019.
58. Gamoudi S, Srasra E. Adsorption of Organic Dyes by HDPy+-Modified Clay: Effect of Molecular Structure on the Adsorption. J Mol Struct. 2019;1193:522–531. https://doi.org/10.1016/j.molstruc.2019.05.055.
59. Piri F, Mollahosseini A, khadir A, Milani Hosseini M. Enhanced Adsorption of Dyes on Microwave-Assisted Synthesized Magnetic Zeolite-Hydroxyapatite Nanocomposite. J Environ Chem Eng. 2019;7(5):103338. https://doi.org/10.1016/j.jece.2019.103338.
60. Wang H, Li Z, Yahyaoui S, Hanafy H, Seliem MK, Bonilla-Petriciolet A, Luiz Dotto G, Sellaoui L, Li Q. Effective Adsorption of Dyes on an Activated Carbon Prepared from Carboxymethyl Cellulose: Experiments, Characterization and Advanced Modelling. Chem Eng J. 2021;417:128116. https://doi.org/10.1016/j.cej.2020.128116.
61. Değermenci GD, Değermenci N, Ayvaoğlu V, Durmaz E, Çakır D, Akan E. Adsorption of Reactive Dyes on Lignocellulosic Waste; Characterization, Equilibrium, Kinetic and Thermodynamic Studies. J Clean Prod. 2019;225:1220–1229. https://doi.org/10.1016/j.jclepro.2019.03.260.